

Mixed-Metal–Organic Framework with Effective Lewis Acidic Sites for Sulfur Confinement in High-Performance Lithium–Sulfur Batteries

Ziqi Wang,[†] Buxue Wang,[†] Yu Yang,[†] Yuanjing Cui,[†] Zhiyu Wang,[†] Banglin Chen,^{*,†,‡} and Guodong Qian^{*,†}

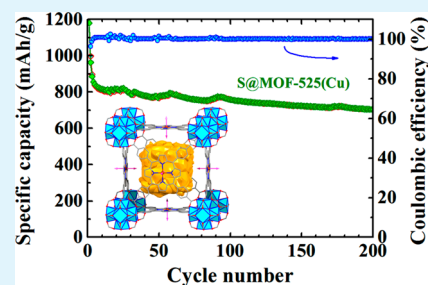
[†]State Key Laboratory of Silicon Materials, Cyrus Tang Center for Sensor Materials and Applications, Department of Materials Science and Engineering, Zhejiang University, Hangzhou 310027 P. R. China

[‡]Department of Chemistry, University of Texas at San Antonio, San Antonio, Texas 78249, United States

Supporting Information

ABSTRACT: The mixed-metal–organic framework approach and a representative zirconium–metalloporphyrin framework (MOF-525) have been developed to create novel sulfur hosts and Li–S batteries. The different local environments at the centers of the porphyrin moieties in a series of MMOFs—MOF-525(2H), MOF-525(FeCl), and MOF-525(Cu)—have led to their different behaviors for the confinement of sulfur and thus Li–S batteries. The unique structure of MOF-525(Cu) has enabled each Cu²⁺ site to offer two Lewis acidic sites, featuring it as a very powerful MOF host for the inclusion of sulfur and polysulfides. The S@MOF-525(Cu) cathode has demonstrated the best performance among all reported sulfur/MOFs composite cathode materials, with a reversible capacity of about 700 mAh/g at 0.5 C after 200 cycles.

KEYWORDS: metal–organic framework, metalloporphyrin ligand, Lewis acidic sites, sulfur confinement, lithium–sulfur battery



INTRODUCTION

Portable devices, such as laptops, mobile phones, digital cameras, and wearable devices, have been widely utilized in our daily life.¹ One of the very important components of this powerful electronic equipment is the rechargeable batteries; it is thus very essential to develop batteries with high energy densities.² Among the diverse rechargeable batteries, traditional lithium ion batteries have been extensively explored; however, they have met their bottleneck due to their low energy densities and specific capacities.³ Lithium–sulfur (Li–S) batteries with a theoretically very high energy density of 2500 Wh/kg and specific capacity of 1675 Ah/kg are very promising for practical applications.⁴ In order to reach such high energy density and specific capacity, a number of scientific issues need to be resolved. One of them is that soluble polysulfides (Li₂S₈, Li₂S₆, Li₂S₄, and Li₂S₃) can dissolve into electrolyte, leading to fast capacity fading and low Coulombic efficiency;^{3,5,6} it is thus very important to restrain polysulfides into the cathode and to diminish their dissolution. Toward this goal, many research endeavors have been pursued. It has been realized that loading sulfur into porous hosts, such as carbonaceous materials,^{7,8} conductive polymers,^{9,10} and porous silica,¹¹ is an effective strategy to improve Li–S battery performance.

Recently, as a new kind of highly porous materials, metal–organic frameworks (MOFs), have been studied as novel sulfur hosts in Li–S battery.^{11–17} MOFs are crystalline materials composed of nodes of metal ions/clusters and organic linkers in infinite arrays.¹⁸ Their pore structures and chemical and

physical properties are designable through changing different metal ions and ligands, which grants their diverse applications in gas storage and separation,^{19,20} detection,²¹ catalysis,^{22–24} biomedicine,²⁵ and photochemical^{18,26} areas. Compared with the most studied carbonaceous materials as sulfur hosts, the pores of MOFs can be decorated with chemically active sites, such as Lewis acidic sites and functional organic groups. These active sites can provide chemical affinities to sulfur and polysulfides in MOFs^{11,12,15,17} that are superior to those of porous carbon materials. MOFs have more capabilities to confine sulfur and polysulfides than porous carbon; however, the developed S/MOF cathodes^{11–17} have still not caught up to the electrochemical performance of the top S/carbon cathodes.^{27–30} This is mainly because of the poor electronic and ionic conductivities of MOFs. The study of S/MOF cathodes is still in its early stages. In order to fully explore the promises of MOF hosts to achieve superior battery performance, the pore structures and properties of MOFs need to be collaboratively accommodated.

To be employed as sulfur hosts in Li–S battery, first of all, MOFs need to be electrochemically stable during cycling to ensure permanent porous structures and thus to confine sulfur and polysulfides inside. Second, pore structures need to be well-designed. Typically, cagelike pores will be better than straight

Received: August 1, 2015

Accepted: September 1, 2015

Published: September 1, 2015

channels for the efficient confinement to sulfur.^{14,17} Third and most importantly, these pores need to offer suitable chemical environments to effectively interact with sulfur and polysulfides. Previous studies have shown that Lewis acidic sites in MOFs such as MIL-100(Cr),¹¹ HKUST-1,¹² ZIF-8,¹⁷ and Ni-MOFs¹⁵ can have chemical interactions with sulfur and polysulfides, both experimentally and theoretically, so their applications in Li–S batteries have been examined. Because the metalloligand approach³¹ can readily incorporate Lewis acidic open metal sites into their porous mixed-metal–organic frameworks (MMOFs), such MMOFs might have some unique feature for their inclusion of sulfur and polysulfides and thus for Li–S batteries. However, such a promise has never been realized. Herein, we report the first example of MMOFs self-assembled from metalloporphyrin ligands as the sulfur host for a Li–S battery displaying a capacity of about 700 mAh/g after 200 cycles at 0.5 C charge/discharge rates.

EXPERIMENTAL SECTION

Material Synthesis. *5,10,15,20-Tetrakis(4-methoxycarbonylphenyl)porphyrin (TPPCOOMe)*. Methyl *p*-formylbenzoate (6.9 g) was dissolved in 100 mL of propionic acid in a 500 mL three-necked flask and stirred under Ar atmosphere for 2 h. Then 3 mL of pyrrole was added dropwise and the mixture was refluxed for 12 h in darkness. The purple crystalline precipitate was collected by filtration and washed with 10 mL of propionic acid and 100 mL of water. TPPCOOMe was obtained by drying the resultant precipitate under vacuum at 60 °C. ¹H NMR (600 MHz, CDCl₃): δ 8.87 (s, 8H), 8.49 (d, 8H), 8.35 (d, 8H), 4.16 (s, 12H).

5,10,15,20-Tetrakis(4-carboxyphenyl)porphyrin (H₂TCPP). KOH (10.0 g) and TPPCOOMe (5.0 g) were dissolved in 160 mL of THF, H₂O, and MeOH in a 1000 mL flask and refluxed for 12 h at 80 °C. When the mixture cooled to room temperature, it was filtered and the filtrate was adjusted to pH 4 with 1.0 M HCl. H₂TCPP solid was collected through filtration, washed with 100 mL of water, and dried in vacuum at 60 °C.

[5,10,15,20-Tetrakis(4-carboxyphenyl)porphyrin]Fe(III) Chloride (FeTCPP). TPPCOOMe (4.0 g), FeCl₂·4H₂O (11.7 g), and 300 mL of THF were loaded into a 500 mL three-necked flask and stirred for 2 h at room temperature. Then the mixture was refluxed at 80 °C for 12 h. After that the solvent was evaporated using a rotary evaporator. The resultant solid was mixed with 15.0 g of KOH and 130 mL of THF, H₂O, and MeOH and refluxed at 80 °C for another 12 h. When the mixture cooled to room temperature, it was filtered and the filtrate was adjusted to pH 4 with 1.0 M HCl. FeTCPP solid was collected through filtration, washed with 100 mL water, and dried in vacuum at 60 °C.

[5,10,15,20-Tetrakis(4-carboxyphenyl)porphyrin]Cu(II) (CuTCPP). TPPCOOMe (2.5 g), CuCl₂·2H₂O (8.8 g), and 300 mL of THF were loaded into a 500 mL three-necked flask and stirred for 2 h at room temperature. Then the mixture was refluxed at 80 °C for 12 h. After that the solvent was evaporated using a rotary evaporator. The resultant solid was mixed with 15.0 g of KOH and 130 mL of THF, H₂O, and MeOH and refluxed at 80 °C for another 12 h. When the mixture cooled to room temperature, it was filtered and the filtrate was adjusted to pH 4 with 1.0 M HCl. CuTCPP solid was collected through filtration, washed with 100 mL of water, and dried in vacuum at 60 °C. Similar ligands and synthesis procedures can also be found in previous reports,^{32,33} and ICP results of the ligands demonstrated that almost 100% of H₂TCPP can be coordinated with Fe(III) or Cu(II) ions.

MOF-525(2H) [MOF-525(FeCl), MOF-525(Cu)]. MOF-525(2H) [MOF-525(FeCl), MOF-525(Cu)] was synthesized according to literature methods.³⁴ Typically, 0.025 g of H₂TCPP (FeTCPP, CuTCPP), 25 mL of acetic acid, and 0.125 g of ZrOCl₂·8H₂O were dissolved in 100 mL of DMF in a 200 mL glass bottle by sonication. Then the bottle was sealed and heated at 65 °C for 3 days. The

resultant solid was collected by centrifuging, washed with DMF and acetone, and activated at 180 °C under vacuum overnight.

S@MOF-525(2H) [S@MOF-525(FeCl), S@MOF-525(Cu)]. Sulfur was loaded into MOF-525(2H) [MOF-525(FeCl), MOF-525(Cu)] host by the melt-diffusion method, as illustrated in Figure 1. Sulfur (0.1 g)

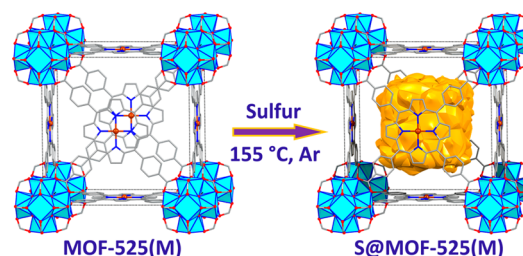


Figure 1. Schematic illustration of S@MOF-525(M) synthesized through the melt-diffusion method at 155 °C under an Ar atmosphere. MOF-525(2H), M = 2H⁺; MOF-525(FeCl), M = Fe³⁺-Cl; MOF-525(Cu), M = Cu²⁺.

and MOF host (0.1 g) were mixed by hand-milling and heated at 60 °C for 12 h in a vacuum oven. Then the oven was filled with Ar and the temperature was raised up to 155 °C and kept there for another 24 h. After cooling to room temperature, S@MOF-525(2H) [S@MOF-525(FeCl), S@MOF-525(Cu)] cathode material was collected.

Battery Assembly. S@MOF-525(2H) [MOF-525(FeCl), MOF-525(Cu)] was mixed with 20 wt % acetylene black and 10 wt % PVDF in NMP, which were coated on Al foil as cathode (~0.7 mg S/cm²). Batteries 2025 were assembled in an Ar-filled glovebox (O₂, H₂O < 1 ppm) with an electrolyte of 1 M LiTFSI in DOL/DME (v:v, 1:1), Celgard 2400 membrane, and Li foil reference anode. Then, 0.1 M LiNO₃ was added to the electrolyte for the purpose of improving battery Coulombic efficiency.

Characterization. ¹H NMR spectra were recorded on a Bruker Advance DMX500 spectrometer (600 MHz) using tetramethylsilane (TMS) as an internal standard. Powder X-ray diffraction (PXRD) data were recorded by a PANalytical X'Pert PRO diffractometer at 40 kV, 25 mA for Cu Kα (λ = 1.541 Å). The SEM morphology and EDS mapping were investigated using Hitachi S4800 field-emission scanning electron microscopy with a HORIBA EMAX energy dispersive spectrometer. Thermogravimetric analysis (TGA) was carried out in a N₂ atmosphere at a scan speed of 10 K/min on a Netzsch TG209 F3 system. X-ray photoelectron spectroscopy (XPS) analysis was performed on a Thermo Scientific Escalab 250Xi instrument with Mg Kα radiation (1253.6 eV) at a scan step of 0.1 eV. Inductively coupled plasma mass spectrometry (ICP-MS) was performed on a Thermo Scientific XSERIES 2 ICP-MS system. The cyclic voltammetry (CV) data were collected with an Arbin electrochemical workstation at a scan rate of 0.1 mV/s between 1.5 and 3.0 V. The charge/discharge profiles, cycle performance, and Coulombic efficiency were obtained with a LAND battery cycler between 1.5 and 3.0 V.

RESULTS AND DISCUSSION

MOF-525(2H) is composed of Zr₆(OH)₄O₄ clusters linked by MTCPP ligand, as shown in Figure S1 (Supporting Information, SI) [MOF-525(2H), M = 2H⁺; MOF-525(FeCl), M = Fe³⁺-Cl; MOF-525(Cu), M = Cu²⁺]. The coordination environment of Zr(IV) atoms in Zr₆(OH)₄O₄ clusters is tightly occupied by O atoms. Unlike Cu(II) atoms of HKUST-1 in paddlewheel clusters, Zr(IV) centers cannot provide accessible Lewis acid sites (LAS). The metal ions at the centers of the porphyrin moieties are chelated by four coplanar N atoms with one or two accessible LAS for the sulfur confinement. To study the effect of LAS on Li–S battery performance, the material without acenter metal sites [MOF-525(2H)] and those with

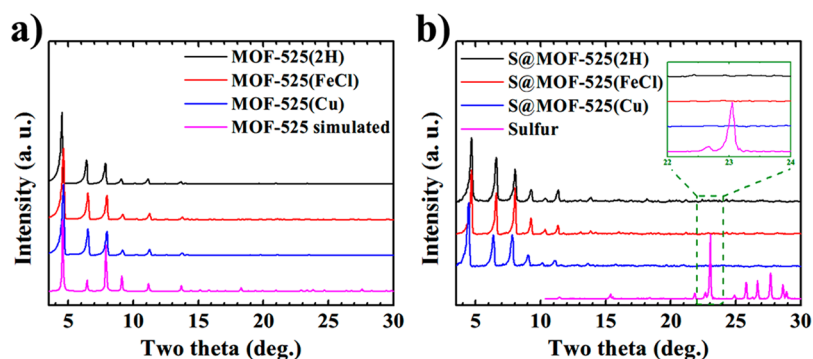


Figure 2. PXRD patterns of (a) as-synthesized MOF-525(2H), MOF-525(FeCl), MOF-525(Cu), and MOF-525 (simulated) and (b) S@MOF-525(2H), S@MOF-525(FeCl), S@MOF-525(Cu), and pristine sulfur with an inset of magnification in the range of 22°–24°.

Fe³⁺-Cl [MOF-525(FeCl)] and Cu²⁺ [MOF-525(Cu)], respectively, have been examined and compared. These MMOFs can accordingly provide zero, one, and two Lewis acidic sites for the binding and inclusion of sulfur, respectively.

Both Fe(III) and Cu(II) were incorporated into MTCPP before the synthesis of MMOFs. MOF-525(2H), MOF-525(FeCl), and MOF-525(Cu) were synthesized under the identical conditions, the phase purities of which were confirmed by PXRD patterns, as displayed in Figure 2a. The experimental PXRDs match with the simulated ones from their X-ray single crystal structures. SEM morphologies in Figure 3 show that the crystals of the MOF-525 series are uniform and exist as cubic-

shaped crystals with a diameter of about 1.8 μm . Sulfur impregnation in MOF hosts was performed through the melt-diffusion method at 155 $^{\circ}\text{C}$, where the liquid sulfur has the lowest viscosity.¹⁴ After heat treatment, these MOF hosts retained their crystalline feature, as indicated by their PXRD patterns in Figure 2b, and their cubic morphologies were not destroyed after an equal amount of sulfur encapsulation, as shown in Figures 3 and S2 (SI, low magnification). Such thermal and chemical stabilities have been established in Zr-based MOFs with Zr₆(OH)₄O₄ clusters.³³ Sulfur ratios in the cathode materials were determined using TGA curves under N₂ atmosphere. In Figure 4, sulfur in S@MOF-525(2H) and S@

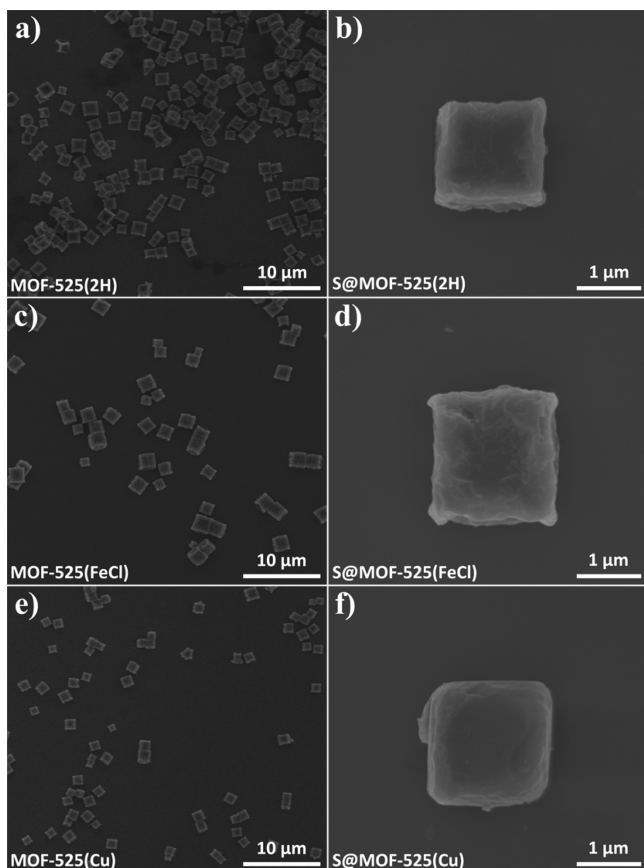


Figure 3. SEM morphologies of the as-synthesized (a) MOF-525(2H), (c) MOF-525(FeCl), and (e) MOF-525(Cu) with sulfur loaded (b) S@MOF-525(2H), (d) S@MOF-525(FeCl), and (f) S@MOF-525(Cu).

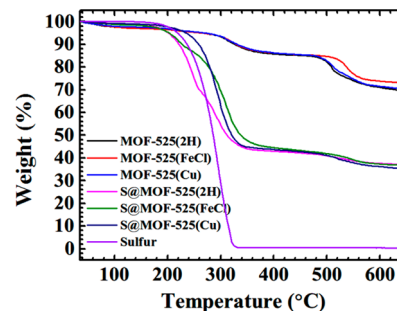


Figure 4. TGA curves under N₂ atmosphere of the as-synthesized MOF-525(2H), MOF-525(FeCl), and MOF-525(Cu); sulfur loaded S@MOF-525(2H), S@MOF-525(FeCl), and S@MOF-525(Cu) cathode materials; and pristine sulfur.

MOF-525(FeCl) shows a two-step weight loss. The first step starts at the same temperature of about 180 $^{\circ}\text{C}$, which is slight lower than that of pristine sulfur (about 190 $^{\circ}\text{C}$); for the second step, S@MOF-525(FeCl) demonstrates a lower beginning temperature than S@MOF-525(2H). The sulfur in S@MOF-525(Cu) features a one-step weight loss, but the beginning temperature (about 210 $^{\circ}\text{C}$) is higher than that of pristine sulfur. Different weight-loss behaviors of the three cathode materials are speculated to be caused by different interactions between sulfur and hosts.¹² TGA indicates that about 50 wt % sulfur is included in the three cathode materials. The sulfur contents match that added during the self-assembly of S@MOF-525(M). This is the maximum loading of S we can achieve experimentally and one of the highest loading amounts among reported S@MOF cathodes.¹⁷ Theoretically, 72 wt % sulfur could be confined in MOF-525 crystals based on the density of liquid sulfur (1.82 g/cm³) and the pore volume of MOF-525 (1.44 cm³/g). Apparently, the unique pore structures

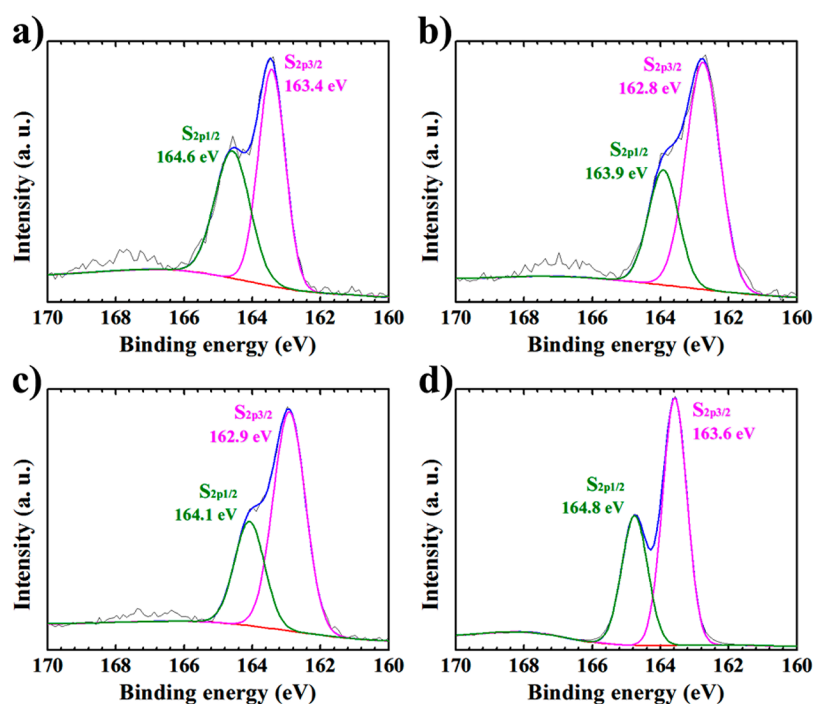


Figure 5. XPS S_{2p} spectra of (a) S@MOF-525(2H), (b) S@MOF-525(FeCl), (c) S@MOF-525(Cu), and (d) pristine sulfur.

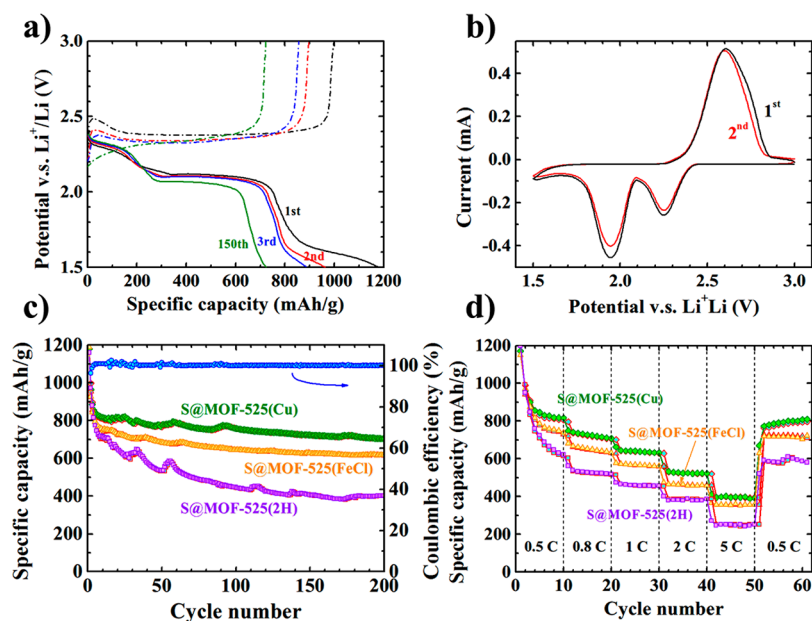


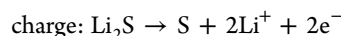
Figure 6. (a) Galvanostatic charge/discharge profiles of S@MOF-525(Cu) at 0.5 C. (b) Cyclic voltammograms of S@MOF-525(Cu) at 0.1 mV/s. (c) Cycle performance of S@MOF-525(2H), S@MOF-525(FeCl), and S@MOF-525(Cu) with the Coulombic efficiency of S@MOF-525(Cu). (d) Rate capability of S@MOF-525(2H), S@MOF-525(FeCl), and S@MOF-525(Cu).

of this MOF-525 series, as demonstrated by their high porosities (BET surface area of about 2600 m^2/g ³⁴) and accessible sites, play a crucial role in the sulfur confinement. The complete sulfur impregnation was further confirmed by the PXRD patterns of the cathode materials. As shown in Figure 2b, no “free” sulfur exists, and all the sulfur has been incorporated into S@MOF-525(M). The homogeneous distribution of sulfur in MOF hosts was confirmed by EDS mappings of the cathode materials, in which Zr and S elements are similarly distributed (Figure S3, SI). As shown in Figure 5, no obvious chemical shift of the S_{2p} spectra was observed in S@

MOF-525(2H) compared with pristine sulfur, while large S_{2p} chemical shifts of about 0.7 eV to a lower energy were observed in S@MOF-525(FeCl) and S@MOF-525(Cu). These significant differences indicate that the Lewis acidic metal sites in S@MOF-525(FeCl) and S@MOF-525(Cu) have strong interactions with sulfur. Such interactions will enforce their confinement to sulfur in hosts and thus to improve the battery performance.

Electrochemical tests were carried out on S@MOF-525(2H), S@MOF-525(FeCl), and S@MOF-525(Cu) to study the effects of LAS in MOF hosts on Li–S battery performance.

Figure 6a displays the galvanostatic charge/discharge profiles of S@MOF-525(Cu) at 0.5 C with a cutoff voltage of 1.5–3 V. It shows the typical Li–S cathode reaction mechanism, which can be generally described as follows:^{3,5}



In the discharge curves, the two plateaus located at 2.3 and 2.1 V correspond to the formation of long-chain polysulfides and short-chain polysulfides, respectively.³⁵ The 2.1 V plateaus dropped only about 0.1 V after 150 cycles, demonstrating the superior electrochemical performance of S@MOF-525(Cu). A small shoulder located at about 1.6 V in the first several cycles is caused by the irreversible deposition of LiNO₃ additive on the cathode.³⁶ In the charge curves, the plateau at about 2.4 V is caused by the transformation of Li₂S and short-chain polysulfides into sulfur.³⁵ Such a reaction mechanism was further characterized by CV curves in Figure 6b. Corresponding to galvanostatic discharge profiles, the potential shift of redox peaks in CV was observed because of the more remarkable polarization phenomenon under the condensed current of the CV test.³⁷ The cycle performances between 1.5 and 3 V at 0.5 C of S@MOF-525(2H), S@MOF-525(FeCl), and S@MOF-525(Cu) are displayed in Figure 6c, showing the reversible capacities of 402, 616, and 704 mAh/g after 200 cycles, respectively. S@MOF-525(2H) suffered fast capacity fading during cycling, while the capacities of S@MOF-525(FeCl) and S@MOF-525(Cu) declined only 0.09% and 0.07% per cycle after the 10th cycle. Rate capabilities of these materials were also investigated, as displayed in Figure 6d. S@MOF-525(FeCl) and S@MOF-525(Cu) have displayed not only high reversible capacities but also good capacity recovery ability, with capacities maintained above 400 mAh/g at 5 C charge/discharge rate. The contribution of the MOF hosts to the capacity of the battery has also been studied, as shown in Figure S4 (SI). When cycling between 1.5 and 3 V, all three MOFs demonstrated a capacity of less than 5 mAh/g, which is negligible compared with the capacity of sulfur. It also indicated that the MOF hosts are electrochemically stable during cycling and capable of providing permanent confinement to sulfur. The electrochemical stability of MOF hosts has also been confirmed by SEM morphologies and PXRD patterns of the 200 times cycled cathodes. In Figure S5 (SI), the cubic structure of the MOF hosts is intact, even if they were cycled for 200 times. PXRD of the 200 times cycled S@MOF-525(Cu) cathode in Figure S6 (SI) demonstrates clear reflection peaks of the MOF hosts, indicating that the crystallinity of the hosts has been maintained after cycling. Obviously, the ultrastable MOF-525 series are superior sulfur hosts than previous reported MOFs, such as ZIF-8, which will decompose with cycling.¹⁴

The battery performance of this MOF-525 series is heavily dependent on their LAS. With two accessible sites per Cu²⁺ metal ion, S@MOF-525(Cu) is the best for the confinement of sulfur, thus demonstrating the best battery performance. Among these three S@MOF-525(M), the MOF-525(2H) performs the worst, because of its deficiency of LAS for the confinement of sulfur. It needs to be pointed out that, compared with previously reported sulfur/MOF composites, the S@MOF-525(Cu) has demonstrated the best cycle performance, as summarized in Figure 7. In the unique structure of MOF-525(Cu), each Cu²⁺ metal ion can offer two LAS, which play a crucial role in its superior performance

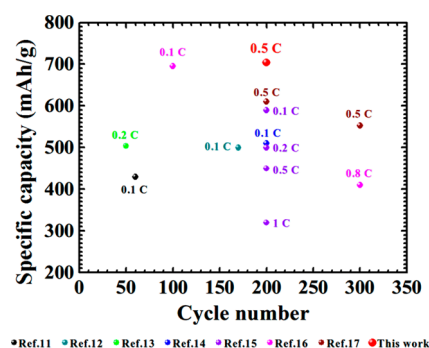


Figure 7. Comparison of the cycle performance of the reported sulfur/MOF composites.

compared to other traditional MOFs, such as HKUST-1,¹² MIL-100(Cr),¹¹ and Ni-MOFs.¹⁵ MOF-525(Cu) also distinguishes itself from those reported MOFs because of its ultrastability, demonstrating its potential applications for Li–S battery.

CONCLUSIONS

In summary, we have developed a mixed-metal–organic framework approach and employed a Cu(II)-embedded zirconium–metalloporphyrin framework MOF-525(Cu) as sulfur host in a Li–S battery. The unique structure of such MMOFs has enabled each Cu²⁺ site within MOF-525(Cu) to offer two Lewis acidic sites. The high porosity of MOF-525(Cu) further enforces its ability to take up more sulfur. The collaborative combination of special open Lewis acidic metal sites and high porosity has featured MOF-525(Cu) as the best MOF host for the sulfur confinement and thus Li–S batteries, to the best of our knowledge. Together with its ultrastability, such a new MMOF host might have potential applications in Li–S batteries. Further development of the design and syntheses of MMOFs will lead to even better MOF hosts for sulfur confinement and thus Li–S batteries in the near future.

ASSOCIATED CONTENT

Supporting Information

The Supporting Information is available free of charge on the ACS Publications website at DOI: 10.1021/acsami.5b07024.

Figures S1–S6, as described in the text (PDF)

AUTHOR INFORMATION

Corresponding Authors

*B.C. e-mail: banglin.chen@utsa.edu.

*G.Q. e-mail: gdqian@zju.edu.cn.

Notes

The authors declare no competing financial interest.

ACKNOWLEDGMENTS

This work was supported by the National Natural Science Foundation of China (Nos. 51272229, 51272231, and 51472217), Zhejiang Provincial Natural Science Foundation of China (No. LR13E020001), and Qianjiang Talent Project (No. QJD1302009). This work is also partially supported by Welch Foundation (AX-1730).

REFERENCES

(1) Yang, Y.; Zheng, G.; Cui, Y. Nanostructured Sulfur Cathodes. *Chem. Soc. Rev.* 2013, 42, 3018–3032.

- (2) Li, Z.; Huang, Y.; Yuan, L.; Hao, Z.; Huang, Y. Status and Prospects in Sulfur–Carbon Composites as Cathode Materials for Rechargeable Lithium–Sulfur Batteries. *Carbon* **2015**, *92*, 41–63.
- (3) Bruce, P. G.; Freunberger, S. A.; Hardwick, L. J.; Tarascon, J. M. Li–O₂ and Li–S Batteries with High Energy Storage. *Nat. Mater.* **2012**, *11*, 19–29.
- (4) Ji, X.; Nazar, L. F. Advances in Li–S Batteries. *J. Mater. Chem.* **2010**, *20*, 9821–9826.
- (5) Manthiram, A.; Fu, Y.; Su, Y. Challenges and Prospects of Lithium–Sulfur Batteries. *Acc. Chem. Res.* **2013**, *46*, 1125–1134.
- (6) Akridge, J. R.; Mikhaylik, Y. V.; White, N. Li/S Fundamental Chemistry and Application to High-Performance Rechargeable Batteries. *Solid State Ionics* **2004**, *175*, 243–245.
- (7) Wang, Z.; Li, X.; Cui, Y.; Yang, Y.; Pan, H.; Wang, Z.; Qian, G. Improving the Performance of Lithium–Sulfur Battery by Blocking Sulfur Diffusing Paths on the Host Materials. *J. Electrochem. Soc.* **2014**, *161*, A1231–A1235.
- (8) Wang, C.; Wan, W.; Chen, J.; Zhou, H.; Zhang, X.; Yuan, L.; Huang, Y. Dual Core-Shell Structured Sulfur Cathode Composite Synthesized by a One-Pot Route for Lithium Sulfur Batteries. *J. Mater. Chem. A* **2013**, *1*, 1716–1723.
- (9) Shao, J.; Li, X.; Zhang, L.; Qu, Q.; Zheng, H. Core-Shell Sulfur@ Polypyrrole Composites as High-Capacity Materials for Aqueous Rechargeable Batteries. *Nanoscale* **2013**, *5*, 1460–1464.
- (10) Fu, Y.; Manthiram, A. Core-Shell Structured Sulfur-Polypyrrole Composite Cathodes for Lithium–Sulfur Batteries. *RSC Adv.* **2012**, *2*, 5927–5929.
- (11) Demir Cakan, R.; Morcrette, M.; Nouar, F.; Davoisne, C.; Devic, T.; Gonbeau, D.; Dominko, R.; Serre, C.; Férey, G.; Tarascon, J. M. Cathode Composites for Li–S Batteries via the Use of Oxygenated Porous Architectures. *J. Am. Chem. Soc.* **2011**, *133*, 16154–16160.
- (12) Wang, Z.; Li, X.; Cui, Y.; Yang, Y.; Pan, H.; Wang, Z.; Wu, C.; Chen, B.; Qian, G. A Metal–Organic Framework with Open Metal Sites for Enhanced Confinement of Sulfur and Lithium–Sulfur Battery of Long Cycling Life. *Cryst. Growth Des.* **2013**, *13*, 5116–5120.
- (13) Bao, W.; Zhang, Z.; Qu, Y.; Zhou, C.; Wang, X.; Li, J. Confine Sulfur in Mesoporous Metal–Organic Framework@Reduced Graphene Oxide for Lithium Sulfur Battery. *J. Alloys Compd.* **2014**, *582*, 334–340.
- (14) Wang, Z.; Dou, Z.; Cui, Y.; Yang, Y.; Wang, Z.; Qian, G. Sulfur Encapsulated ZIF-8 as Cathode Material for Lithium–Sulfur Battery with Improved Cyclability. *Microporous Mesoporous Mater.* **2014**, *185*, 92–96.
- (15) Zheng, J.; Tian, J.; Wu, D.; Gu, M.; Xu, W.; Wang, C.; Gao, F.; Engelhard, M. H.; Zhang, J.; Liu, J.; Xiao, J. Lewis Acid–Base Interactions between Polysulfides and Metal Organic Framework in Lithium Sulfur Batteries. *Nano Lett.* **2014**, *14*, 2345–2352.
- (16) Zhao, Z.; Wang, S.; Liang, R.; Li, Z.; Shi, Z.; Chen, G. Graphene Wrapped Chromium-MOF(MIL-101)/Sulfur Composite for Performance Improvement of High-Rate Rechargeable Li–S Batteries. *J. Mater. Chem. A* **2014**, *2*, 13509–13512.
- (17) Zhou, J.; Li, R.; Fan, X.; Chen, Y.; Han, R.; Li, W.; Zheng, J.; Wang, B.; Li, X. Rational Design of a Metal–Organic Framework Host for Sulfur Storage in Fast, Long-Cycle Li–S Batteries. *Energy Environ. Sci.* **2014**, *7*, 2715–2724.
- (18) Cui, Y.; Yue, Y.; Qian, G.; Chen, B. Luminescent Functional Metal–Organic Frameworks. *Chem. Rev.* **2012**, *112*, 1126–1162.
- (19) Xiang, S.; Zhou, W.; Zhang, Z.; Green, M. A.; Liu, Y.; Chen, B. Open Metal Sites within Isostructural Metal–Organic Frameworks for Differential Recognition of Acetylene and Extraordinarily High Acetylene Storage Capacity at Room Temperature. *Angew. Chem., Int. Ed.* **2010**, *49*, 4615–4618.
- (20) Liu, Y.; Eubank, J. F.; Cairns, A. J.; Eckert, J.; Kravtsov, V. C.; Luebke, R.; Eddaoudi, M. Assembly of Metal–Organic Frameworks (MOFs) Based on Indium-Trimer Building Blocks: A Porous MOF with soc Topology and High Hydrogen Storage. *Angew. Chem., Int. Ed.* **2007**, *46*, 3278–3283.
- (21) Chen, B.; Xiang, S.; Qian, G. Metal–Organic Frameworks with Functional Pores for Recognition of Small Molecules. *Acc. Chem. Res.* **2010**, *43*, 1115–1124.
- (22) Wang, C.; deKrafft, K. E.; Lin, W. B. Pt Nanoparticles@ Photoactive Metal–Organic Frameworks: Efficient Hydrogen Evolution via Synergistic Photoexcitation and Electron Injection. *J. Am. Chem. Soc.* **2012**, *134*, 7211–7214.
- (23) Li, S.; Xu, Q. Metal-organic Frameworks as Platforms for Clean Energy. *Energy Environ. Sci.* **2013**, *6*, 1656–1683.
- (24) Alkordi, M. H.; Liu, Y.; Larsen, R. W.; Eubank, J. F.; Eddaoudi, M. Zeolite-like Metal–Organic Frameworks as Platforms for Applications: On Metalloporphyrin-Based Catalysts. *J. Am. Chem. Soc.* **2008**, *130*, 12639–12641.
- (25) An, J.; Geib, S. J.; Rosi, N. L. Cation-Triggered Drug Release from a Porous Zinc–Adeninate Metal–Organic Framework. *J. Am. Chem. Soc.* **2009**, *131*, 8376–8377.
- (26) Chen, Y.; Ma, S. Q. Microporous Lanthanide Metal–Organic Frameworks. *Rev. Inorg. Chem.* **2012**, *32*, 81–100.
- (27) Xin, S.; Gu, L.; Zhao, N.; Yin, Y.; Zhou, L.; Guo, Y.; Wan, L. Smaller Sulfur Molecules Promise Better Lithium–Sulfur Batteries. *J. Am. Chem. Soc.* **2012**, *134*, 18510–18513.
- (28) Song, J.; Yu, Z.; Xu, T.; Chen, S.; Sohn, H.; Regula, M.; Wang, D. Flexible Freestanding Sandwich-Structured Sulfur Cathodes with Superior Performance for Lithium–Sulfur Batteries. *J. Mater. Chem. A* **2014**, *2*, 8623–8627.
- (29) Kim, J.; Lee, D.; Jung, H.; Sun, Y.; Hassoun, J.; Scrosati, B. An Advanced Lithium–Sulfur Battery. *Adv. Funct. Mater.* **2013**, *23*, 1076–1080.
- (30) Elazari, R.; Salitra, G.; Garsuch, A.; Panchenko, A.; Aurbach, D. Sulfur-Impregnated Activated Carbon Fiber Cloth as a Binder-Free Cathode for Rechargeable Li–S Batteries. *Adv. Mater.* **2011**, *23*, 5641–5644.
- (31) Das, M. C.; Xiang, S.; Zhang, Z.; Chen, B. Functional Mixed Metal–Organic Frameworks with Metalloligands. *Angew. Chem., Int. Ed.* **2011**, *50*, 10510–10520.
- (32) Feng, D.; Jiang, H.; Chen, Y.; Gu, Z.; Wei, Z.; Zhou, H. Metal–Organic Frameworks Based on Previously Unknown Zr₆/Hf₈ Cubic Clusters. *Inorg. Chem.* **2013**, *52*, 12661–12667.
- (33) Feng, D.; Gu, Z.; Li, J.; Jiang, H.; Wei, Z.; Zhou, H. Zirconium-Metalloporphyrin PCN-222: Mesoporous Metal–Organic Frameworks with Ultrahigh Stability as Biomimetic Catalysts. *Angew. Chem., Int. Ed.* **2012**, *51*, 10307–10310.
- (34) Morris, W.; Voloskiy, B.; Demir, S.; Gándara, F.; McGrier, P. L.; Furukawa, H.; Cascio, D.; Stoddart, J. F.; Yaghi, O. M. Synthesis, Structure, and Metalation of Two New Highly Porous Zirconium Metal–Organic Frameworks. *Inorg. Chem.* **2012**, *51*, 6443–6445.
- (35) Zhang, S. S. Liquid Electrolyte Lithium/Sulfur Battery: Fundamental Chemistry, Problems, and Solutions. *J. Power Sources* **2013**, *231*, 153–162.
- (36) Zhang, S. S.; Read, J. A. A New Direction for the Performance Improvement of Rechargeable Lithium/Sulfur Batteries. *J. Power Sources* **2012**, *200*, 77–82.
- (37) Ryu, H.; Park, J.; Park, J.; Ahn, J.; Kim, K.; Ahn, J.; Nam, T.; Wang, G.; Ahn, H. High Capacity Cathode Materials for Li–S Batteries. *J. Mater. Chem. A* **2013**, *1*, 1573–1578.